Critical Role of TNF-α-Induced Macrophage VEGF and iNOS Production in the Experimental Corneal Neovascularization

Peirong Lu,[*,1–3] *Longbiao Li,*[1] *Gaoqin Liu,*[1] *Tomohisa Baba,*[3] *Yuko Ishida,*[4] *Mizuho Nosaka,*[4] *Toshikazu Kondo,*[4] *Xueguang Zhang,*[2] *and Naofumi Mukaida*[*,3]

Purpose. We evaluated the roles of tumor necrosis factor (TNF)-α in alkali-induced corneal neovascularization (CNV).

Methods. CNV was induced by alkali injury and compared in wild-type (WT) BALB/c mice, and TNF receptor 1-deficient (TNF-Rp55 KO) counterparts, or in mice treated with TNF-α antagonist and recombinant TNF-α. Angiogenic factor expression and leukocyte accumulation in the early phase after injury were quantified by real-time PCR and immunohistochemical analysis, respectively.

Results. Alkali injury augmented the intraocular mRNA expression of TNF-α and its receptor, together with a transient macrophage and neutrophil infiltration. Compared to WT mice, TNF-Rp55 KO mice exhibited reduced CNV. Intraocular F4/80-positive macrophages and Ly-6G-positive neutrophils infiltration did not change in KO mice compared to WT mice after the injury. Alkali injury induced a massively increased intraocular mRNA expression of angiogenic factors, including vascular endothelial growth factor (VEGF), inducible nitric oxide synthase (iNOS), interleukin (IL)-6, E-selectin, and intercellular adhesion molecule (ICAM)-1 in WT mice, whereas these increments were retarded severely in KO mice. Immunofluorescence analysis demonstrated that F4/80-positive cells expressed VEGF and iNOS. Moreover, TNF-α enhanced VEGF and iNOS expression by peritoneal macrophage from WT, but not KO mice. Topical application of TNF-α antagonist reduced CNV, while topical application of recombinant TNF-α enhanced it.

Conclusions. TNF-Rp55-KO mice exhibited impaired alkali-induced CNV through reduced intracorneal infiltrating macrophage VEGF and iNOS expression. (*Invest Ophthalmol Vis Sci.* 2012;53:3516–3526) DOI:10.1167/iovs.10-5548

The cornea is characterized by an absence of blood vessels under physiological conditions.[1] Corneal avascularity is essential to visual acuity, and depends on the balance between angiogenic and anti-angiogenic molecules.[2–6] Corneal neovascularization (CNV) arises from various causes, including corneal infections, misuse of contact lenses, chemical burns, and inflammation,[7–9] and frequently can lead to impaired vision. Before the onset of CNV, a large number of neutrophils and, to a lesser degree, monocytes/macrophages infiltrate into the cornea. We proved previously that experimental CNV can occur independently of granulocyte infiltration.[10] Moreover, we observed that infiltrated macrophages exert complicated roles, by using different chemokine receptor signals in the development of CNV.[11–13]

A proinflammatory cytokine, tumor necrosis factor-α (TNF-α), is produced by a variety of cell types, including neutrophils, macrophages, lymphocytes, and endothelial cells.[14] TNF signals through two distinct cell surface receptors, TNF-receptor (TNF-R)p55, and TNF-Rp75. TNF-Rp55 mediates the major biological activities of TNF-α.[15] Based on their essential roles in inflammatory responses, anti-TNF-α mAbs or TNF antagonists have been used to treat inflammatory ocular diseases and uveitis.[16]

Although evidence is accumulating to indicate the essential roles of the TNF-α-TNF-Rp55 axis in inflammatory responses, the involvement of this axis in angiogenesis is defined poorly. Saika et al. observed that alkali-induced CNV was more severe in TNF-α-deficient mice than wild-type (WT) controls.[17] They demonstrated further that endogenous TNF-α can counteract the activities of transforming growth factor (TGF)-β and vascular endothelial growth factor (VEGF) on vascular endothelial cells, thereby inhibiting corneal neovascularization.[18] On the contrary, TNF-α can induce endothelial cell migration in vitro and angiogenesis in vivo, when implanted into corneas, chorioallantoic membranes, or sponge implants.[19–22] In line with these observations, Shi et al. reported that a TNF antagonist, etanercept, and TNF antibody reduced laser-induced choroidal neovascularization.[23] An anti-TNF mAb, infliximab, was reported to be effective against age-related macular degeneration (AMD),[24] which is characterized by choroidal neovascularization. These conflicting observations prompted us to investigate further the roles of TNF-α on ocular neovascularization, by using a frequently used ocular neovascularization model, alkali injury-induced CNV.[4–6,10–13]

From the [1]Department of Ophthalmology and [2]Clinical Immunology Key Laboratory of Jiangsu Province, the First Affiliated Hospital of Soochow University, Suzhou City, China; the [3]Division of Molecular Bioregulation, Cancer Research Institute, Kanazawa University, Kanazawa, Japan; and the [4]Department of Forensic Medicine, Wakayama Medical University, Wakayama, Japan.

Supported by International Cooperative Program of Kanazawa University (NM), National Natural Science Foundation in China (NSFC) Grants 30771978 and 30972712(NSFC) Grants 30771978 and 30972712, Qing-Lan Project of Education Bureau of Jiangsu Province, and Jiangsu Province's Key Medical Talents Program Grant RC2011104 (PL).

Submitted for publication March 19, 2010; revised September 26, 2010, March 8, June 7, August 8, and December 4, 2011, and March 27, 2012; accepted April 15, 2012.

Disclosure: **P. Lu**, None; **L. Li**, None; **G. Liu**, None; **T. Baba**, None; **Y. Ishida**, None; **M. Nosaka**, None; **T. Kondo**, None; **X. Zhang**, None; **N. Mukaida**, None

*Each of the following is a corresponding author: Peirong Lu, Clinical Immunology Key Laboratory of Jiangsu Province, the First Affiliated Hospital of Soochow University, 188 Shizi Street, Suzhou 215006, China PR; lupeirong@yahoo.com.hk.

Naofumi Mukaida, Division of Molecular Bioregulation, Cancer Research Institute, Kanazawa University, 13-1 Takara-machi, Kanazawa 920-0934, Japan; naofumim@kenroku.kanazawa-u.ac.jp.

Investigative Ophthalmology & Visual Science, June 2012, Vol. 53, No. 7

Materials and Methods

Reagents and Antibodies

A specific TNF antagonist, etanercept, was purchased from Wyeth Pharmaceutical (Osaka, Japan). Recombinant mouse interferon (IFN)-γ (catalog No. 485-MI/CF) and mouse VEGF ELISA Kit (MMV00) were obtained from R&D Systems (Minneapolis, MN). Rat anti-mouse F4/80 (clone A3-1) mAb was acquired from Serotec (Oxford, UK). Rat anti-mouse CD31 (MEC13.3), anti-mouse-Ly-6G (Clone IA8, catalog No. 551495) mAbs, and rabbit anti-inducible nitric oxide synthase (iNOS) (catalog No. 610332) polyclonal antibodies, were purchased from BD Pharmingen (San Diego, CA). Rabbit anti-mouse TNF-α (ab34674) and anti-mouse TNF-Rp55 (ab19139) polyclonal antibodies were supplied by Abcam (Cambridge, UK). Goat anti-mouse VEGF (sc-1836) polyclonal antibodies were from Santa Cruz Biotechnology (Santa Cruz, CA). VECTASHIELD Mounting medium with DAPI (H-1200) was obtained from Vector Laboratories (Burlingame, CA). Recombinant mouse TNF-α and IL-1β, and neutralizing rabbit anti-mouse TNF-α IgG were prepared as described previously.[25] Lipopolysaccharide (LPS, Cat No. L8274) was purchased from Sigma-Aldrich Chemical Co. (St. Louis, MO). Alexa Fluor 594 or 488-labeled donkey anti-rat IgG Ab, Alexa Fluor 594 or 488-labeled donkey anti-rabbit IgG Ab, and donkey anti-goat IgG Ab were purchased from Invitrogen Life Technologies (Carlsbad, CA).

Mice

Pathogen-free BALB/c mice were obtained from Clea Japan (Yokohama, Japan), and were designated as WT mice in the present experiments. TNF-Rp55-deficient mice were backcrossed to BALB/c mice from eight to 10 generations,[26,27] and bred under specific pathogen-free conditions at the Animal Research Center of Kanazawa University (Kanazawa, Japan). Seven- to 8-week-old male mice were used for the experiments. All animal experiments were performed under specific pathogen-free conditions in the Institute for Experimental Animals, Kanazawa University, in accordance with the ARVO Statement for the Use of Animals in Ophthalmic and Vision Research, and complied with the standards set out in the Guidelines for the Care and Use of Laboratory Animals of Kanazawa University.

Alkali-Induced Corneal Injury Model

Corneal injury was induced by placing a 2-mm filter disc saturated with 1 N NaOH onto the left eye of the mouse for 45 seconds as described previously.[10–13] TNF-α, etanercept, and anti-TNF-α antibodies were dissolved in 0.2% sodium hyaluronate (Sigma-Aldrich) immediately before the topical application. In some experiments, the alkali-treated eyes received 5 μL of TNF-α antagonist preparation dissolved in 0.2% sodium hyaluronate at a concentration of 0.5 or 1 mg/mL, or 5 μL of 0.2% sodium hyaluronate as vehicle twice a day for 7 days immediately after the alkali injury. In another series of experiments, the eyes were treated with alkali for 40 seconds, and received 5 μL of recombinant mouse TNF-α preparation or neutralizing rabbit anti-mouse TNF-α IgG at a concentration of 100 μg/mL, or 5 μL of 0.2% sodium hyaluronate as vehicle twice a day for 7 days immediately after the alkali injury. At the indicated time intervals, mice were sacrificed and whole eyes were removed. The eyes were snap-frozen in ornithine carbamoyltransferase (OCT) compound for histological analysis, or the corneas were removed and placed immediately into RNALate (Qiagen, Tokyo, Japan) and kept at −86°C until total RNA extraction was performed. Each experiment was repeated at least three times.

Histological and Immunohistochemical Analysis

The OCT-embedded tissues were cut into 8-μm thick slices, and the fixed cryosections then were subjected to hematoxylin and eosin staining. The sections were incubated overnight at 4°C with rat anti-mouse F4/80 antibody (1 μg/mL) and rat anti-mouse-Ly-6G (2.5 μg/mL) to identify macrophages and neutrophils, respectively. Tissue sections then were incubated with biotin-conjugated anti-rat immunoglobulin antibodies as secondary antibodies. Other sets of sections were incubated overnight at 4°C with rabbit anti-TNF-α, rabbit anti-TNF-Rp55, and goat anti-VEGF pAbs, to detect TNF-α, TNF-Rp55, and VEGF expression, respectively. These slides were incubated with biotin-conjugated anti-rabbit or anti-goat immunoglobulin antibodies as the secondary antibodies. The immune complexes were detected by using an ABC kit and a DAB Substrate Kit from Vector Laboratories, Inc. according to the manufacturer's instructions. Slides then were counterstained with hematoxylin and mounted. The numbers of F4/80- or Ly-6G-positive cells were counted at 200-fold magnification in five randomly chosen fields of corneal sections from each animal,[11–13] by an examiner with no prior knowledge of the experimental procedures. The numbers of positive cells per mm^2 were calculated.

A Double-Color Immunofluorescence Analysis

A double-color immunofluorescence analysis was performed to determine VEGF or iNOS expression by infiltrating macrophages. Briefly, the fixed cryosections (8 μm thick) were incubated with PBS containing 10% normal donkey serum and 1% BSA to reduce nonspecific reactions. Thereafter, the sections were incubated with the combinations of rat anti-Ly-6G and goat anti-VEGF, rat anti-F4/80 and goat anti-VEGF, rat anti-F4/80 and rabbit anti-iNOS, or rabbit anti-TNF-α and goat anti-VEGF Abs overnight at 4°C. After being rinsed with PBS, for a double-immunofluorescence analysis using anti-VEGF, the sections then were incubated with a combination of Alexa Fluor 594 donkey anti-rat IgG and Alexa Fluor 488 donkey anti-goat IgG (1/100) for 45 minutes at room temperature in the dark. For double-immunofluorescence analyses to detect macrophage iNOS expression, the sections were incubated further with the combination of Alexa Fluor 594 donkey anti-rat IgG and Alexa Fluor 488 donkey anti-rabbit IgG (1/100) for 45 minutes at room temperature in the dark. For double-immunofluorescence analyses using anti-TNF-α and anti-VEGF, the sections were incubated further with the combination of Alexa Fluor 594 donkey anti-rabbit IgG and Alexa Fluor 488 donkey anti-goat IgG (1/100) for 45 minutes at room temperature in the dark. Finally, the sections were washed with PBS and mounted with VECTASHIELD Mounting medium with DAPI, and immunofluorescence was visualized with a fluorescence microscope (Olympus, Tokyo, Japan). Images were processed by using graphics software (Adobe Photoshop, version 7.0; Adobe, Mountain View, CA).

Enumeration of Corneal Neovascularization

Corneal whole mount staining was performed and blood vessels in the corneas were measured according to previous reports.[2,28] Corneal flat mounts were rinsed in PBS, fixed in acetone, rinsed in PBS, blocked in 2% BSA, stained with rat anti-mouse CD31 (1:100; BD Pharmingen) at 4°C overnight, and washed, and the corneas then were incubated with Alexa Fluor 594 or Alexa Fluor 488 donkey anti-rat IgG (1/100) for 2 hours at room temperature in the dark and analyzed by microscope. Digital pictures of the flat mounts were taken. Then, the area covered by CD31 was measured morphometrically on these flat mounts using NIH Image software (National Institutes of Health, Bethesda, MD). The total corneal area was outlined using the innermost vessel of the limbal arcade as the border. The total area of neovascularization then was normalized to the total corneal area, and the percentage of the cornea covered by vessels calculated. In another series of experiments, the fixed cryosections (8 μm thick) were stained with rat anti-mouse CD31 (1:100; BD Pharmingen) at 4°C overnight, washed, and then incubated with biotin-conjugated anti-rat immunoglobulin antibody as secondary antibodies. The immune complexes were detected by using an ABC kit and a DAB Substrate Kit from Vector Laboratories, Inc. according to the manufacturer's instructions. Slides then were counterstained with hematoxylin and mounted. The numbers and sizes of the CNV were determined as described previously,[11–13] by an examiner with no

Table 1. Specific Sets of Primers of Real-Time PCR

Gene Names	Primer Sequences
TNF-α	(F) TCTTCTGTCTACTGAACTTCGGGGTGA
	(R) GTGGTTTGCTACGACGTGGGCTA
TNF-Rp55	(F) TGCGGTGCTGTTGCCCCTGGTTAT
	(R) CTTTCCAGCCTTCTCCTCTTTGA
VEGF	(F) CGCCGCAGGAGACAAACCGAT
	(R) ACCCGTCCATGAGCTCGGCT
bFGF	(F) AAGAGCGACCCACACGTCAAAC
	(R) GTAACACACTTAGAAGCCAGCAGCC
TGF-β	(F) GCTGACCCCCACTGATACGCCT
	(R) CTGTCACAAGAGCAGTGAGCGC
TSP-1	(F) GCAGACACAGACAAAAACGGGGAG
	(R) TCTCCAACCCCATCCATGTCCG
iNOS	(F) AACCCCTTGTGCTGTTCTCAGCC
	(R) GTGGACGGGTCGATGTCACATGC
IL-6	(F) TGATGCTGGTGACAACCACGGC
	(R) TAAGCCTCCGACTTGTGAAGTGGTA
E-selectin	(F) GGCCAGCGCAGGTTGAATGC
	(R) ATGTTGCCCTGCTGTGGCGC
ICAM-1	(F) CCGGTCCTGACCCTGAGCCA
	(R) 5-ATTGGACCTGCGGGGTGGGT
IL-1α	(F) TCAGCAACGTCAAGCAACGGGA
	(R) AGGTGCTGATCTGGGTTGGATGGT
IL-1β	(F) AAAGCCTCGTGCTGTCGGACC
	(R) CCTTTGAGGCCCAAGGCCACA
CCL2	(F) CACAGTTGCCGGCTGGAGCA
	(R) TTGGGACACCTGCTGCTGGT
β-actin	(F) CAGGAGATGGCCACTGCCGCAT
	(R) AAGAGCCTCAGGGCATCGGAAC

F, forward primer; R, reverse primer.

knowledge of the experimental procedures. Briefly, images were captured with a digital camera and imported into Adobe Photoshop. Then, the numbers of neovascular tubes per mm^2, and the proportions of CNV in the hot spots were determined using NIH Image analysis software.[11–13] Most sections were taken from the central region of the cornea. The numbers and areas of corneal neovascularization were evaluated on at least two sections from each eye.

RNA Isolation and Real-Time PCR

Total RNAs were extracted from the corneas or cultured macrophages with the use of RNeasy Mini Kit (Qiagen). The resultant RNA preparations were treated further with ribonuclease-free deoxyribonuclease (DNase) I (Life Technologies Inc., Gaithersburg, MD) to remove genomic DNA. The PCR solution contained 2 μL cDNA, the specific primer set (0.2 μM final concentration), and 12.5 μL of SYBR *Premix Ex Taq*™ (SYBR *Premix Ex Taq* Perfect Real Time PCR Kit; Takara) in a final volume of 25 μL. The sequences of the PCR primer pairs are listed in the Table. Quantitative PCR was performed on iCycler iQ Multi-Color Real Time PCR Detection System (170-8740; Bio-Rad, Shanghai, China). PCR parameters were initial denaturation at 95°C for 1 minute, followed by 40 circles of 95°C for 5 seconds, and 60°C for 30 seconds. mRNA expression was normalized to the levels of β-actin mRNA.

Isolation and Culture of Murine Peritoneal Macrophages

Peritoneal macrophages from WT or TNF-Rp55 KO mice were obtained as described previously.[11,12] The cells were suspended in antibiotic-free RPMI medium containing 10% fetal bovine serum (FBS), and incubated in a humidified incubator at 37°C in 5% CO_2 in 6-well cell culture plates (Nalge Nunc International Corp., Naperville, IL). Two hours later, nonadherent cells were removed, and the medium was replaced. The cells then were stimulated with the indicated concentrations of murine TNF-

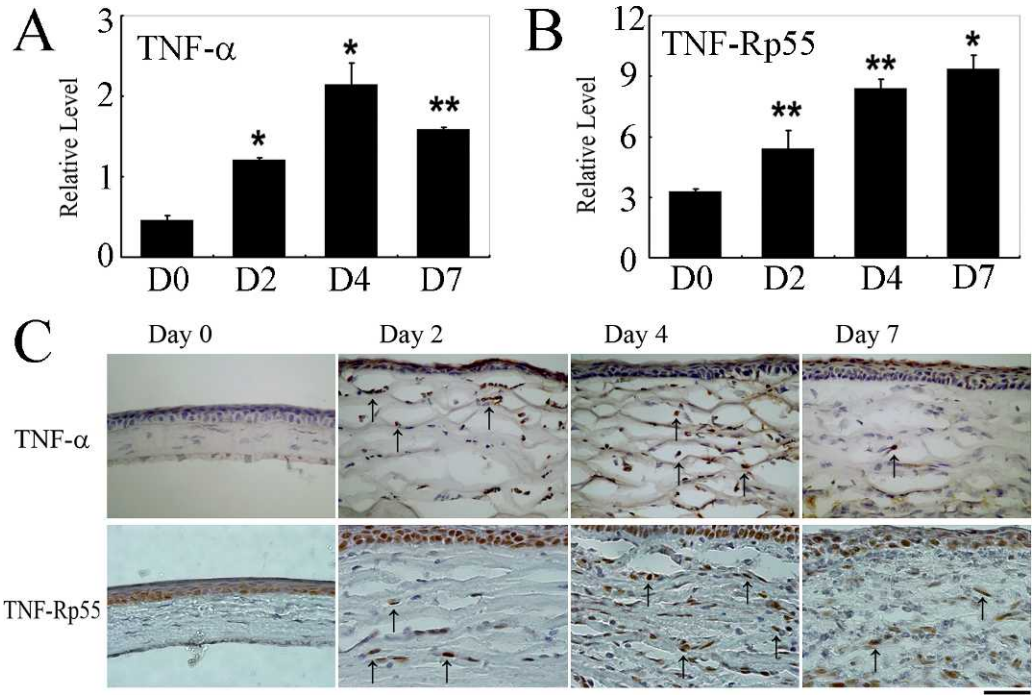

Figure 1. The expression of TNF-α and its receptor, TNF-Rp55, in cornea after alkali injury. Real-time PCR was conducted to detect TNF-α (**A**) and TNF-Rp55 (**B**) mRNA normalized to the levels of β-actin mRNA as described in Materials and Methods, and are shown with mean ± SEM. Representative results from 3 independent experiments are shown. $^{*}P < 0.05$; $^{**}P < 0.01$ vs. D0. (**C**) Whole eyes were obtained at 0, 2, 4, and 7 days after alkali injury, and processed for immunohistochemical analysis using anti-TNF-α (*upper panels*) and anti-TNF-Rp55 (*lower panels*) antibodies. Representative results from 3–5 animals of each time point are shown. *Arrows* indicate the positive cells. Original magnification ×400. Scale bar 50 μm.

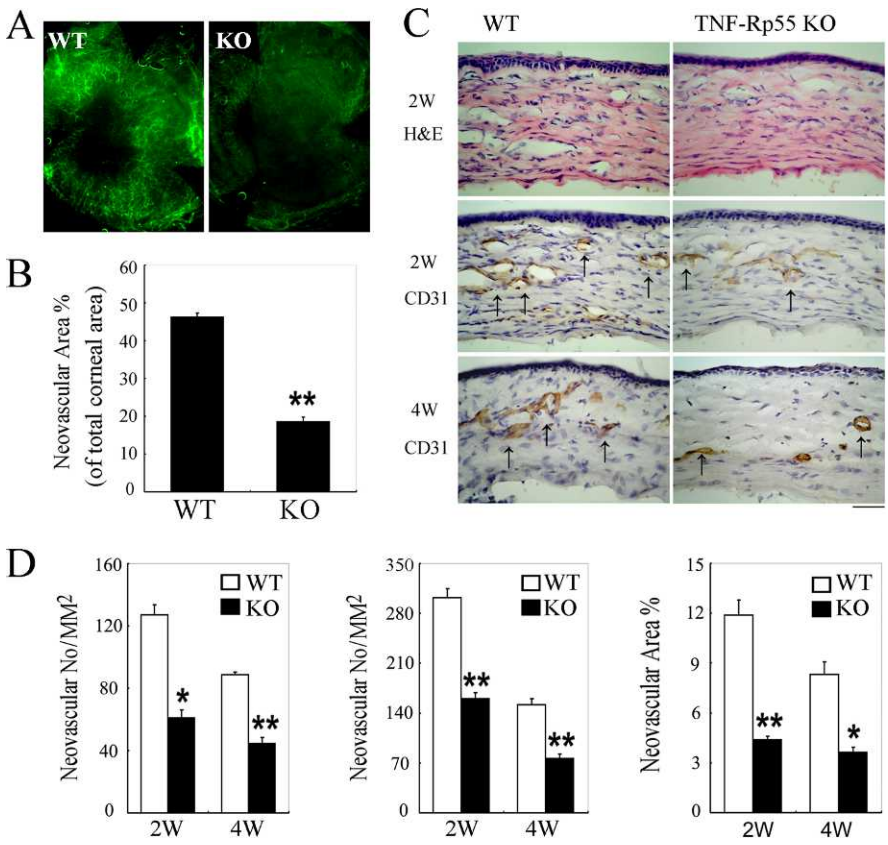

Figure 2. Alkali-induced CNV. (**A**) Representative photographs of corneal flat mounts of WT (*left panel*) and TNF-Rp55-deficient (*right panel*) mice 2 weeks after alkali injury, stained by anti-CD31 antibodies to visualize blood vessels. Original magnification ×25. (**B**) Neovascularized corneal area of total corneal area percent measured by whole mount staining 2 weeks after alkali injury. Value represents mean and SEM ($n = 5$–7 animals). $^{**}P <$ 0.01. (**C**) Corneal tissues were obtained at 2 and 4 weeks after the injury from WT (*left panels*) and TNF-Rp55-deficient (*right panels*) mice. Tissues were stained with hematoxylin and eosin staining (*upper panels*) or immunostained with anti-CD31 antibodies (*middle and lower panels*), and representative results from three independent experiments are shown. *Arrows* indicate the CD31-positive newly formed vessels. Original magnification ×400. Scale bar 50 μm. (**D**) CNV numbers per mm^2 in whole section (*left panel*), CNV numbers per mm^2 in hot spots (*middle panel*), and percent CNV areas in hot spots (*right panel*) were determined on corneas obtained from WT or KO mice 2 and 4 weeks after the injury. Each value represents mean and SEM ($n = 5$ animals). $^{*}P < 0.05$; $^{**}P < 0.01$ WT versus TNF-Rp55 KO mice.

α for 12 hours or the indicated concentrations of LPS, IFN-γ or IL-1β for 24 hours. Total RNAs were extracted from the cultured cells and subjected to real-time PCR as described above. In another series of experiments, murine macrophages were seeded onto 12-well-plates at 5×10^5 cells/well. After adhesion, the cells were stimulated with the indicated concentrations of murine TNF-α for 12 hours in a 37°C incubator with 5% CO_2. Supernatants were collected to determine VEGF concentrations using a Mouse VEGF ELISA Kit (R&D Systems), according to the manufacturer's instructions.

Statistical Analysis

The means and SEM were calculated for all parameters determined in the study. Data were analyzed statistically using one-way ANOVA, or two-tailed Student's *t*-test. A value of $P < 0.05$ was considered statistically significant.

Results

Intracorneal Expression of TNF-α, and its Receptor, TNF-Rp55 after Alkali-Induced Corneal Injury

We first examined the expression of TNF-α and its receptor, TNF-Rp55, in corneas after alkali-induced corneal injury. TNF-α mRNA barely was detectable in untreated eyes, but was increased markedly after alkali injury (Fig. 1A). Concomitantly, TNF-α protein was detected immunohistochemically in infiltrating cells after alkali injury, but not in untreated eyes (Fig. 1C, upper panels). Moreover, alkali injury augmented markedly the mRNA expression of TNF-Rp55 (Fig. 1B). Furthermore, immunohistochemical analysis demonstrated that the infiltrated leukocytes and corneal epithelial cells expressed TNF-Rp55 (Fig. 1C, lower panels). The enhanced intracorneal expression of TNF-α and TNF-Rp55 suggests the possible involvement of the TNF-α-TNF-Rp55 interactions in alkali-induced CNV.

Impaired Alkali-Induced CNV in TNF-Rp55 KO Mice

We next explored the effects of genetic ablation of TNF-Rp55 on alkali-induced CNV. CNV was evident macroscopically in WT mice 2 weeks after the injury, consistent with our previous reports.[11–13] CNV at 2 weeks after the injury was attenuated significantly in TNF-Rp55 KO mice compared to those of WT mice as evidenced by corneal whole mount method (Figs. 2A, 2B). Immunohistochemical analysis using anti-CD31 antibodies revealed similar tendencies in WT and TNF-Rp55 KO mice even at microscopic levels (Figs. 2C, 2D). These observations indicate that the TNF-α-TNF-Rp55 axis was indispensable for alkali-induced CNV.

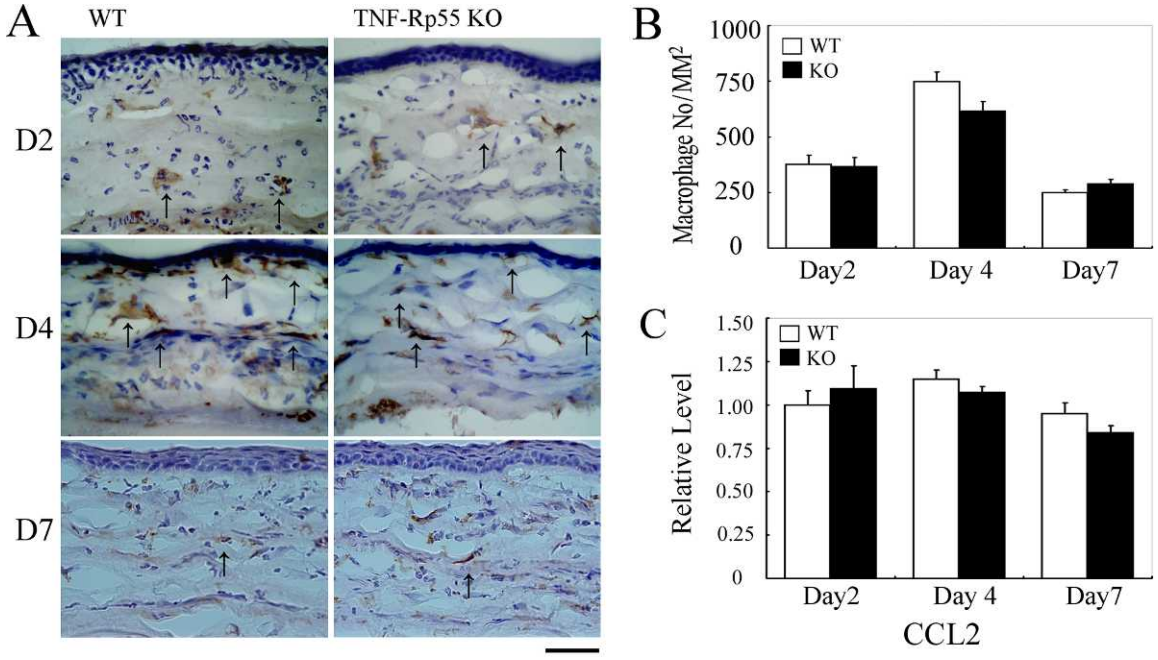

Figure 3. Macrophage recruitment in the injured corneas of WT and TNF-Rp55-deficient mice. (**A**) Corneal tissues were obtained from WT mice (*left panels*) and TNF-Rp55-deficient mice (*right panels*), two days (*upper panels*), four days (*middle panels*), and seven days (*lower panels*) after the injury. Tissues were immunostained with rat anti-F4/80 mAb. Representative results from 5 individual animals are shown. *Arrows* indicate the positive cells. Original magnification ×400. Scale bar 50 μm. (**B**) The numbers of infiltrated F4/80-positive macrophages were determined, as described in Materials and Methods, and the mean and SEM are shown here ($n = 5$). The data were judged as statistically insignificant when compared between WT and TNF-Rp55 KO mice. (**C**) The mRNA of CCL2 to β-actin of WT (*black bars*) and TNF-Rp55-deficient mice (*open bars*) were determined by quantitative RT-PCR analysis. Values represent means and SEM ($n = 3$–5 animals).

Marginal Effects of TNF-Rp55 Deficiency on Alkali Injury-Induced Intraocular Leukocyte Infiltration

We observed previously that Ly-6G-positive granulocytes and F4/80-positive macrophages infiltrated injured corneas, reaching their peak levels 2 and 4 days after the injury in WT mice, respectively.[11–13] Monocytes/macrophages can be a rich source of angiogenic factors,[29–33] while infiltrated granulocytes have few roles in alkali-induced CNV.[10] Hence, we examined the effects of TNF-Rp55 deficiency on macrophage and granulocyte infiltration into the wounded corneas. Rare F4/80-positive macrophages were observed in untreated corneas as observed previously.[11] Ly-6G-positive granulocytes (data not shown) and F4/80-positive macrophages infiltrated into corneas to similar extents in WT mice compared to TNF-Rp55 KO mice after the injury (Fig. 3). We observed further that mRNA of a major macrophage-tropic chemokine, CCL2, was enhanced in corneas of WT and TNF-Rp55 KO mice to similar extents after alkali injury (Fig. 3C). Thus, the lack of TNF-Rp55 has few apparent effects on the intraocular infiltration of leukocytes in the present alkali injury-induced CNV, probably because it has few effects on the expression of a potent macrophage-tropic chemokine, CCL2.

Reduced Pro-Angiogenic and Adhesion Molecule Expression in TNF-Rp55 KO Mice after Alkali Injury

The balance between angiogenic and anti-angiogenic factors determines the outcome of angiogenesis processes in various situations. Hence, we examined the mRNA expression of angiogenic and anti-angiogenic factors in corneas after alkali injury. Alkali injury increased intraocular mRNA expression of an angiogenic factor, TGF-β, and an anti-angiogenic molecule, thrombospondin (TSP)-1 in WT and TNF-Rp55 KO mice to similar extents (Fig. 4). After alkali injury, WT mice exhibited augmented intraocular mRNA expression of other potent angiogenic molecules, including VEGF, basic fibroblast growth factor (bFGF), iNOS, interleukin (IL)-6, and adhesion molecules, E-selectin and intercellular adhesion molecule (ICAM)-1, and the enhanced expression of these molecules was attenuated markedly in TNF-Rp55 KO mice (Fig. 4). On the contrary, the expression of IL-1α and IL-1β was enhanced to similar extents in WT and KO mice. Consistently with our previous observations,[10] immunohistochemical analysis demonstrated that infiltrating leukocytes and repopulating epithelial cells after alkali injury expressed VEGF in the early phase (Fig. 5A). A double immunofluorescence analysis demonstrated that infiltrating macrophages (Fig. 5B), but not the Ly-6G-positive granulocytes, mainly expressed VEGF. Moreover, double-color immunofluorescence analysis detected the cells expressing simultaneously VEGF and TNF-α (Fig. 5B), indicating that the infiltrating macrophages expressed VEGF and TNF-α. We further revealed that F4/80-positive macrophage also expressed iNOS (Fig. 5B). Thus, intraocularly infiltrated macrophages expressed VEGF and iNOS, two potent angiogenic molecules.

Enhanced VEGF and iNOS Expression by Murine Macrophages with TNF-α Stimulation

We observed that alkali injury enhanced intracorneal TNF-α mRNA expression to similar extents in WT and TNF-Rp55 KO mice (Fig. 4). Hence, we next examined the effects of TNF-α on the expression of VEGF and iNOS. TNF-α enhanced markedly the mRNA expression of VEGF and iNOS by peritoneal macrophages from WT mice in a dose-dependent manner (Figs. 6A, 6B). Moreover, TNF-α augmented VEGF

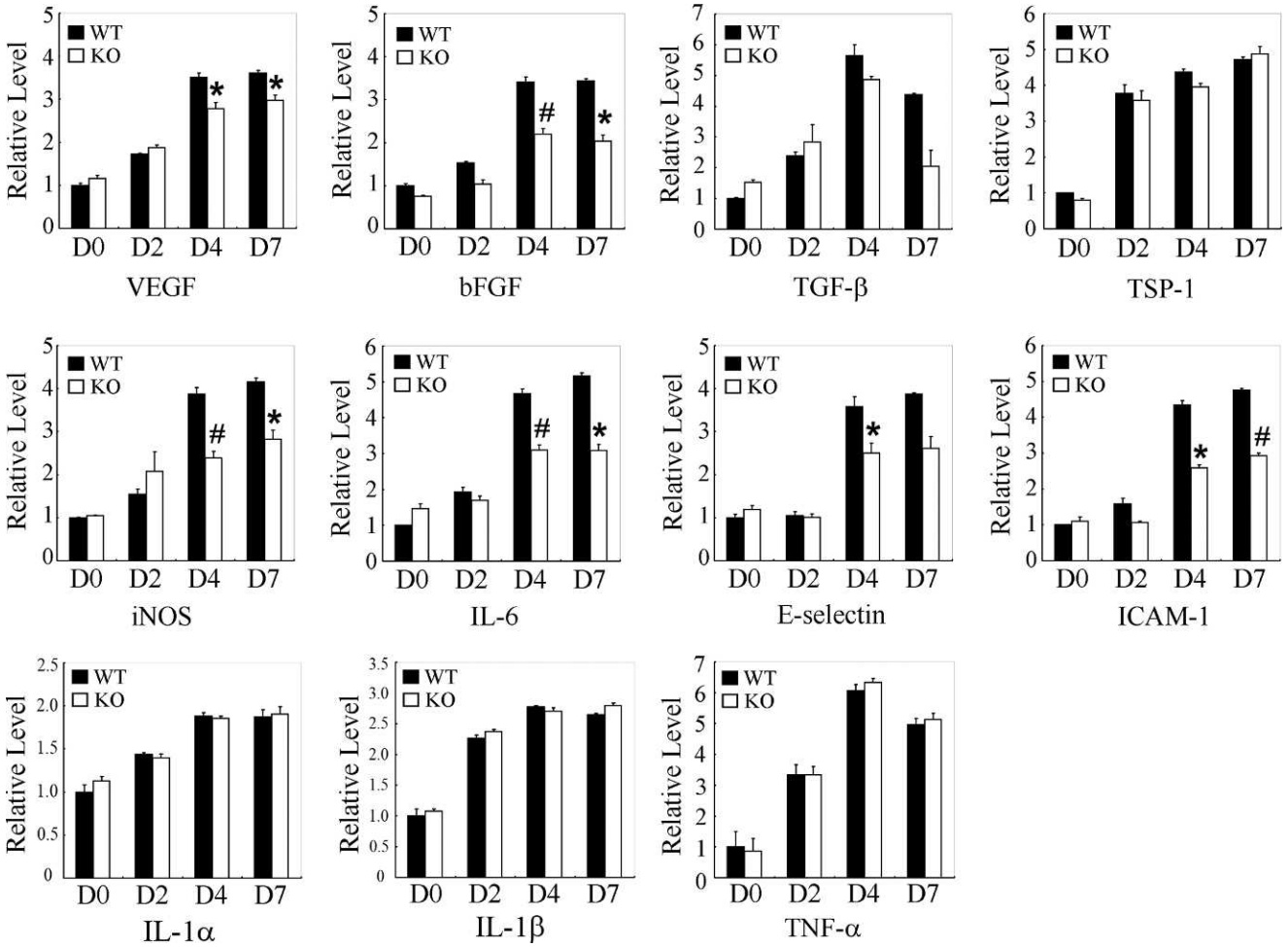

Figure 4. Quantitative RT-PCR analysis of pro-angiogenic and anti-angiogenic gene expression in the injured corneas of WT and TNF-Rp55 KO mice. Representative results from three independent experiments are shown. The mRNAs of VEGF, bFGF, TGF-β, TSP-1, iNOS, IL-6, E-selectin, ICAM-1, IL-1α, IL-1β, and TNF-α to β-actin of WT (*black bars*) and TNF-Rp55-deficient mice (*open bars*) were determined as described in Materials and Methods. All values represent means and SEM ($n = 3$–5 animals). $^{*}P < 0.05$; $^{\#}P < 0.01$ WT versus KO mice.

protein production by macrophages (Fig. 6C), but TNF-Rp55 deficiency abrogated the responsiveness of macrophages to TNF-α in terms of VEGF and iNOS expression (Figs. 6A–C). Moreover, the intracorneal numbers of VEGF and F4/80 double-positive macrophages were reduced in TNF-Rp55 KO mice compared to WT mice after injury (Fig. 5B). However, LPS, IFN-γ, or IL-1β induced WT- or TNF-Rp55 KO-derived macrophages to express VEGF or bFGF to similar extents (Figs. 6D–F), indicating that TNF-Rp55 deficiency did not impair the capacity of macrophages to express VEGF or bFGF as a whole. These observations would indicate that TNF-α can induce macrophages to express potent angiogenic molecules, VEGF, iNOS, and bFGF, solely through the interaction with TNF-Rp55.

Effects of TNF-α and its Inhibitors on Alkali-Induced CNV

The genetic deletion of TNF-Rp55 gene may have compound effects on the phenotypes observed after alkali injury. To exclude this possibility, we first examined the effects of topical application of TNF-α antagonist, etanercept, on alkali-induced CNV of WT mice. Etanercept reduced alkali-induced CNV level compared to control mice (Fig. 7). Because etanercept is a fusion protein between the extracellular portion of human TNF-Rp75 and human IgG Fc portion, it can block TNF-α and TNF-β.[16] To clarify the roles of TNF-α more definitively, we next examined the effects of recombinant mouse TNF-α or neutralizing anti-mouse TNF-α topical application on alkali-induced CNV of WT mice. Topical administration of mouse recombinant TNF-α enhanced alkali-induced CNV when it was administered locally in the early phase after alkali injury at the concentration of 100 μg/mL (Fig. 8). Neutralizing anti-mouse TNF-α consistently attenuated alkali-induced CNV when given topically in the early phase after alkali injury (Fig. 8). These observations indicate further that TNF-α may promote alkali-induced CNV by activating the infiltrated macrophages to produce potent angiogenic factors, VEGF and iNOS.

Discussion

TNF-α is a proinflammatory cytokine produced by a variety of cell types including neutrophils, macrophages, lymphocytes, and endothelial cells.[14] There are two distinct types of TNF receptors, TNF-Rp55 and TNF-Rp75. TNF-Rp55 is expressed ubiquitously by most types of cells, whereas TNF-Rp75 usually is restricted to some cell types and its expression should be induced.[16] Thus, most of its biologic activities are mediated by TNF-Rp55.[15,16]

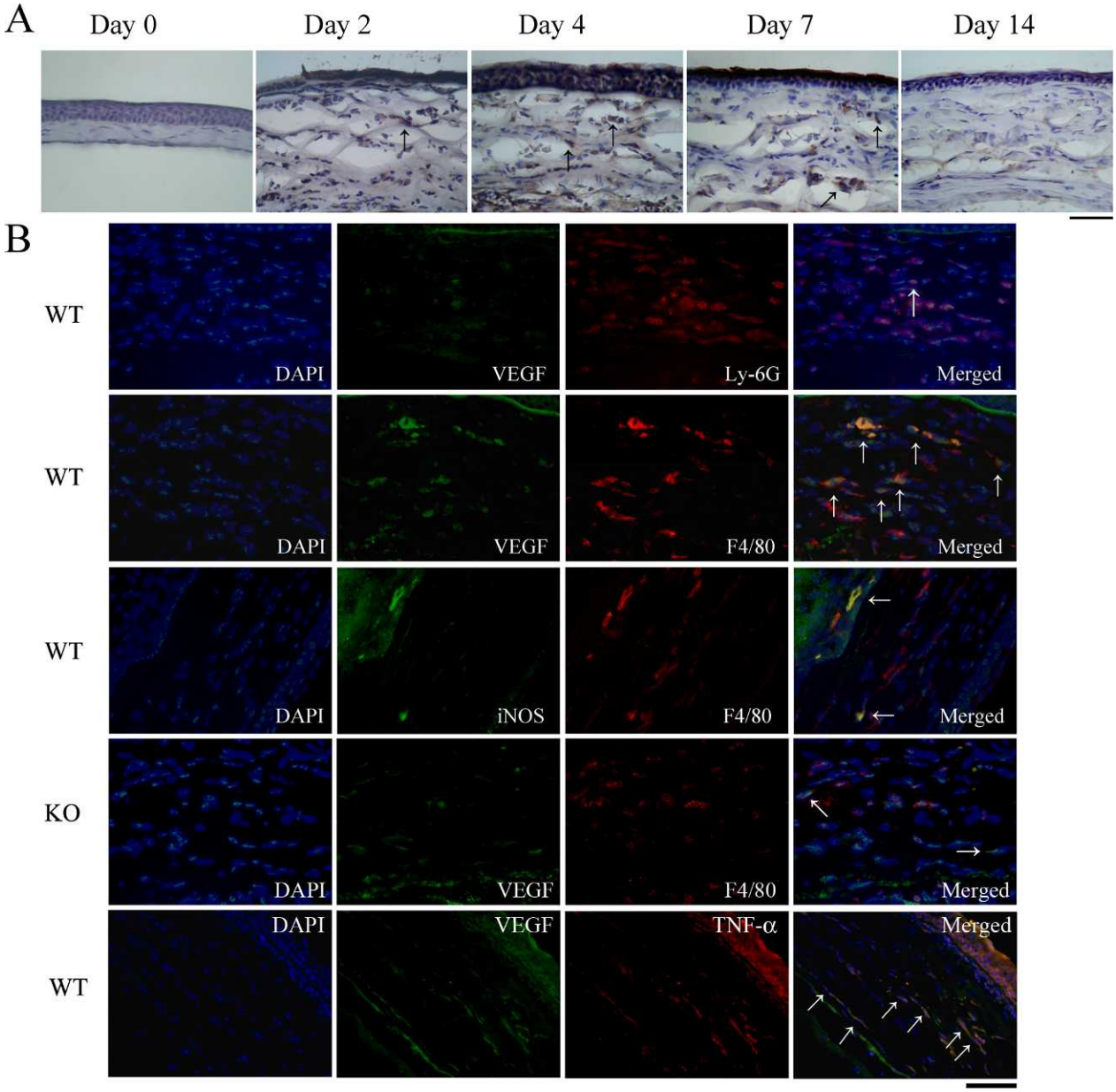

Figure 5. **(A)** Whole eyes were obtained at the indicated time intervals after alkali injury and processed for immunohistochemical analysis using anti-VEGF antibodies. Representative results from four individual animals are shown. **(B)** Double-color immunofluorescence analysis of VEGF or iNOS expression on F4/80-positive macrophages or Ly-6G-positive granulocytes, or TNF-α and VEGF expression from corneas 4 days after the injury. The samples were immunostained with combinations of anti-VEGF and anti-Ly-6G, anti-VEGF and anti-F4/80, anti-iNOS and anti-F4/80, or anti-TNF-α and anti-VEGF antibodies, as described in Materials and Methods, and observed with fluorescence microscopy. Signals were merged digitally in the right panels. Representative results from 5 individual animals are shown. *Arrows* indicate the double-positive cells. Original magnification ×400. Scale bar 50 μm.

The roles of TNF-α in neovascularization remain elusive. This cytokine can induce endothelial cell migration in vitro, and angiogenesis in vivo, when implanted into corneas, chorioallantoic membranes, or sponge implants.[19–22] In contrast, the deficiency of *TNF-α* gene can aggravate ocular neovascularization after alkali injury or central cauterization.[17,18] TNF-Rp55 KO mice exhibited no abnormalities in physiologic retinal neovascularization, but showed defects in pathologic retinal neovascularization.[34] We observed that a higher dose of TNF-α (500 μg/mL) did not have any apparent effects on alkali-induced CNV when applied topically (data not shown). Thus, the effects of TNF-α may be dependent on its local concentration, exposure duration, and the type and growth state of the target cells.[35,36]

These discrepancies prompted us to define the roles of the TNF-α-TNF-Rp55 axis in alkali-induced CNV. Here, we demonstrated that genetic ablation of *TNF-Rp55* gene, and the administration of TNF antagonist or anti-TNF-α, attenuated alkali-induced CNV. Moreover, in contrast to the effects of a higher dose of TNF-α (500 μg/mL), topical administration of mouse TNF-α (100 μg/mL) aggravated alkali-induced CNV. These results were inconsistent with the previous observation on TNF-α-deficient mice.[17,18] These discrepancies may be explained by the differences in the mouse strains used in the

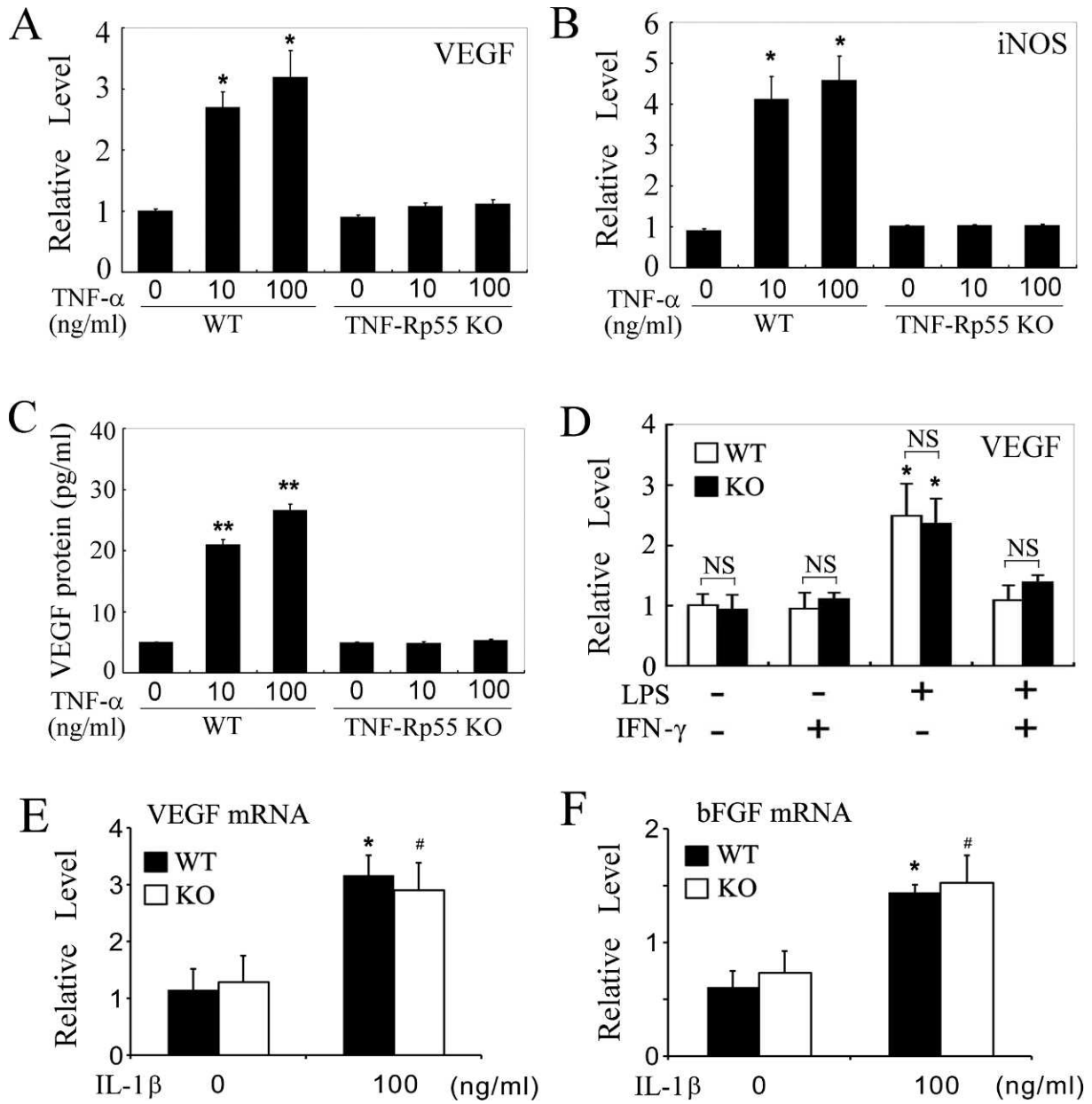

Figure 6. VEGF and iNOS expression by murine peritoneal macrophages from WT mice or TNF-Rp55 KO mice after stimulation. (**A**) and (**B**) Real-time PCR was conducted as described in Materials and Methods. Representative results of macrophage VEGF (**A**) and iNOS (**B**) expression normalized to the levels of β-actin mRNA after recombinant TNF-α stimulation from three independent experiments are shown here. (**C**) Murine macrophages were stimulated with the indicated concentrations of TNF-α for 12 hours. VEGF production in the supernatants was detected with ELISA as described in Materials and Methods. (**D**) Real-time PCR results of macrophage VEGF expression normalized to the levels of β-actin mRNA after 24 hours of IFN-γ (500 U/mL), LPS (100 ng/mL), or the combination of LPS and IFN-γ stimulation. The representative results from three independent experiments are shown. Each value represents the mean and SEM ($n = 3$). $^{*}P < 0.05$; $^{**}P < 0.01$ compared to untreated. NS, no significant difference for WT versus KO mice. (**E**) and (**F**) Real-time PCR results of macrophage VEGF and bFGF expression normalized to the levels of β-actin mRNA after 24 hours of IL-1β (100 ng/mL) stimulation. All values represent means ± SEM ($n = 6$ experiments). $^{*}P < 0.05$, versus untreated WT macrophages; $^{\#}P < 0.05$ versus untreated KO macrophages.

previous studies[17,18] and our present work. Moreover, in the previous study, expression of other TNF-related genes, and the effects of TNF antagonists or anti-TNF-α antibodies were not examined. Thus, it cannot be excluded that genetic ablation of *TNF-α* gene can result in augmentation of TNF-β expression. If so, augmented TNF-β expression can induce neovascularization by acting on TNF-Rp55. On the contrary, if a higher dose of TNF-α might reduce TNF-β expression by a negative feedback mechanism, reduced TNF-β expression might negate the effects of TNF-α.

Normal corneas lack any vasculature, and physiological corneal avascularity is maintained by the net balance between pro-angiogenic and anti-angiogenic factors.[2–6] Alkali treatment increased the expression of angiogenic factors, VEGF, bFGF, TGF-β, IL-6, and iNOS, as well as E-selectin and ICAM-1, the adhesion molecules that have crucial roles in ocular neovascularization.[37,38] Except TGF-β, the augmented expression of the angiogenic factors and adhesion molecules was depressed in TNF-Rp55-deficient mice compared to WT mice. On the contrary, the expression of a potent anti-angiogenic factor,

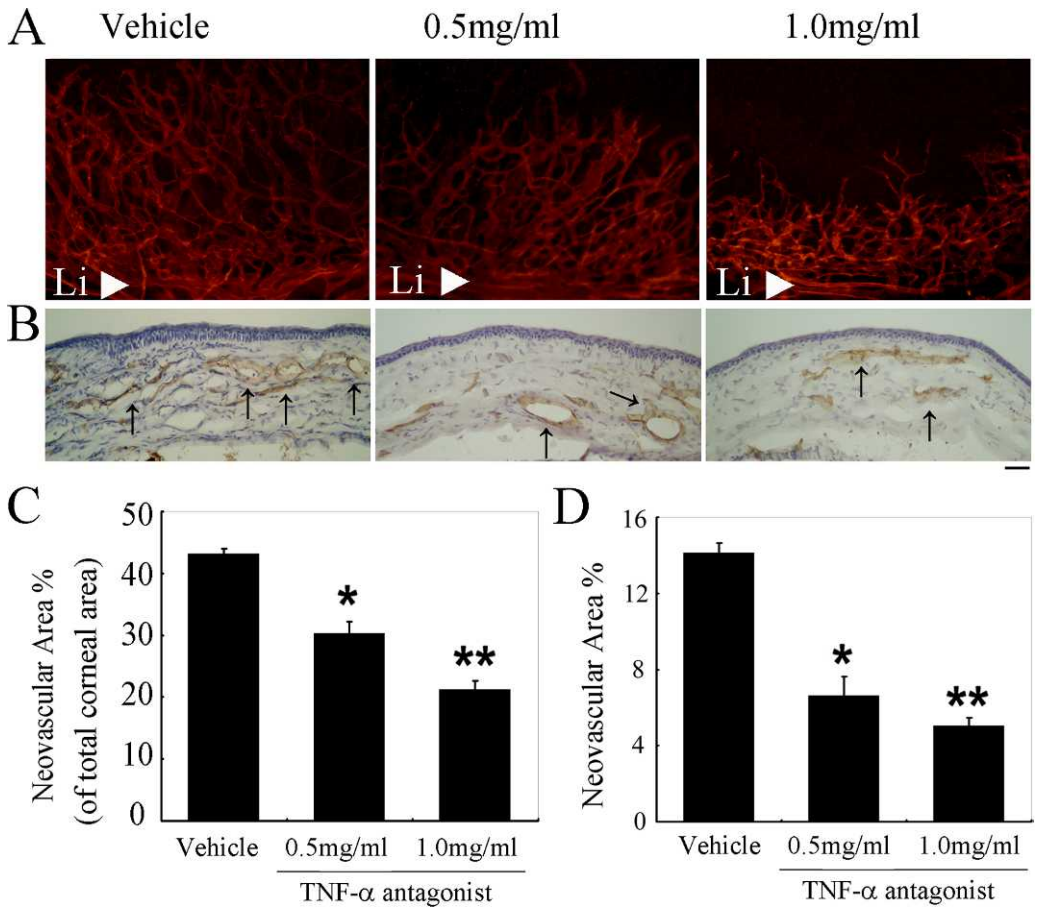

Figure 7. The effects of topical TNF-α antagonist application on CNV. (**A**) Representative CNV of WT mice applied topically with TNF-α antagonist, at 2 weeks after alkali injury, as shown by the CD31-positive areas in the corneal flat mounts (Li, limbal vascular arcade). Original magnification ×100. Representative results from five animals from each group are shown. (**B**) Corneal tissues were obtained two weeks after the injury from WT mice applied topically with TNF-α antagonist or vehicle, and were immunostained with anti-CD31 antibody. Representative results from three independent experiments are shown. *Arrows* indicate the CD31-positive newly formed vessels. Original magnification ×200. Scale bar 50 μm. (**C**) and (**D**) The CNV area measured by corneal whole mount staining (**C**), while percent CNV areas in hot spots measured by immunohistochemical staining from corneal cryosections (**D**) were determined. Each value represents mean and SEM ($n = 5$ animals). $^{*}P < 0.05$; $^{**}P < 0.01$ compared to vehicle.

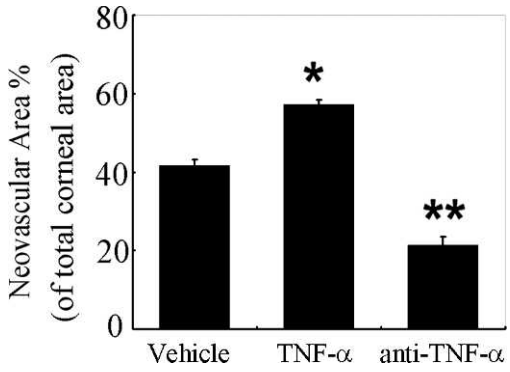

Figure 8. The effects of topical TNF-α and anti-TNF-α application on CNV. Neovascularized corneal area of total corneal area percent of WT mice applied topically with TNF-α or anti-TNF-α at 2 weeks after alkali injury measured by whole mount staining. Each value represents mean and SEM. Representative results from 5–7 animals from each group are shown here. $^{*}P < 0.05$; $^{**}P < 0.01$ compared to vehicle. Our study demonstrates that TNF-Rp55-KO exhibited impaired alkali-induced corneal neovascularization through reduced expression of VEGF and iNOS by infiltrating macrophages. Anti-TNF therapy may be useful as an angiogenic regulator for treating corneal diseases that exhibit neovascularization.

TSP-1, was increased to a similar extent in WT and TNF-Rp55 KO mice. Thus, it is likely that TNF-α induced CNV by augmenting the expression of angiogenic factors and adhesion molecules.

Several lines of evidence indicate that macrophages can be pro-angiogenic by producing angiogenic factors in ocular neovascularization.[29–33] TNF-α and IL-1 can activate similar intracellular signaling pathways, such as NF-κB and AP-1, and can induce the expression of chemokines and adhesion molecules, which are presumed to have crucial roles in the recruitment of leukocytes, including monocytes/macrophages. We recently observed that IL-1ra-deficient mice exhibited enhanced intracorneal macrophage recruitment after alkali injury.[39] Thus, enhanced IL-1 signal can augment macrophage recruitment. Actually, we found that alkali injury increased intraocular IL-1α and IL-1β mRNA expression in WT and TNF-Rp55 KO mice to similar extents. Moreover, similar observations were obtained on mRNA expression of CCL2, a chemokine crucially involved in macrophage infiltration. We assumed at first that TNF-α may promote neovascularization by inducing macrophage recruitment as we observed in the colon carcinogenesis model.[40] In contrast to our expectation, absence of *TNF-Rp55* gene did not reduce alkali injury-induced intracorneal macrophage infiltration, probably due to sustained CCL2 expression. Thus, the TNF-α-TNF-Rp55 interactions did

not have apparent profound effects on the infiltration of macrophages, a rich source of angiogenic factors, in this model.

We observed that intraocularly infiltrated F4/80-positive macrophages expressed two potent angiogenic factors, VEGF and iNOS. Lee et al. reported that TNF-α can stimulate macrophage to express VEGF.[41] Likewise, we observed that TNF-α induced murine peritoneal macrophages from WT, but not TNF-Rp55-deficient mice, to express VEGF and iNOS. Consistently, VEGF expression was depressed in TNF-Rp55 KO-derived F4/80-positive macrophages compared to WT-derived ones. Moreover, because we detected TNF-Rp55 mRNA expression in murine peritoneal macrophages (data not shown), these observations would indicate that the TNF-α-TNF-Rp55 axis is crucial to VEGF and iNOS production by TNF-Rp55-expressing macrophages. However, TNF-Rp55 deficiency failed to abrogate CNV completely, suggesting the contribution of other mediators to CNV. The candidate molecules may be IL-1α and IL-1β, because IL-1α and IL-1β can induce the expression of VEGF and bFGF to similar levels in WT and TNF-Rp55 KO-mouse-derived macrophages. This assumption is supported further by the observation that alkali injury enhanced, to similar extents, their intracorneal expression in WT and TNF-Rp55 KO mice.

Double-color immunofluorescence analysis revealed that the infiltrating F4/80-positive macrophages expressed VEGF and TNF-α. M1 macrophages are a main producer of TNF-α, while M2 macrophages can promote angiogenesis by producing VEGF.[42] However, in selected pathological conditions, mixed types of macrophage phenotypes have been observed,[42] particularly in resolution phase of tissue injury.[43] As we conducted double-color immunofluorescence analysis 4 days after the injury, when corneal lesions were in resolution phase, M1-M2 mixed types of macrophages can be detected in the cornea.

Corneal epithelial cell migration also is indispensable to healing after alkali injury by suppressing inflammatory corneal angiogenesis.[28] Okada et al. observed that TNF-α inhibited corneal epithelial cell migration.[44] Thus, decreased TNF-α signal in TNF-Rp55-deficient mice can promote epithelial cell migration, and eventually reduce CNV.

Corneal clarity is necessary for normal vision. Corneal neovascularization frequently can lead to loss of corneal transparency and impaired vision. Our study demonstrates that TNF-Rp55-KO exhibited impaired alkali-induced CNV through reduced expression of VEGF and iNOS by infiltrating macrophages. Moreover, we observed that the treatment with TNF-α antagonist or anti-TNF-α antibodies significantly decreased alkali-induced mouse corneal neovascularization. Thus, anti-TNF therapy may be useful as an angiogenic regulator for treating corneal diseases that exhibit neovascularization. However, this requires further investigation.

References

1. Ambati BK, Nozaki M, Singh N, et al. Corneal avascularity is due to soluble VEGF receptor-1. *Nature*. 2006;443:993–997.
2. Cursiefen C, Masli S, Ng TF, et al. Roles of thrombospondin-1 and -2 in regulating corneal and iris angiogenesis. *Invest Ophthalmol Vis Sci*. 2004;45:1117–1124.
3. Gao G, Ma J. Tipping the balance for angiogenic disorders. *Drug Discov Today*. 2002;7:171–172.
4. Zhang SX, Ma JX. Ocular neovascularization: implication of endogenous angiogenic inhibitors and potential therapy. *Prog Retin Eye Res*. 2007;26:1–37.
5. Edelman JL, Castro MR, Wen Y. Correlation of VEGF expression by leukocytes with the growth and regression of blood vessels in the rat cornea. *Invest Ophthalmol Vis Sci*. 1999;40:1112–1123.
6. Lai CM, Spilsbury K, Brankov M, Zaknich T, Rakoczy PE. Inhibition of corneal neovascularization by recombinant adenovirus mediated antisense VEGF RNA. *Exp Eye Res*. 2002;75:625–634.
7. Chang JH, Gabison EE, Kato T, Azar DT. Corneal neovascularization. *Curr Opin Ophthalmol*. 2001;12:242–249.
8. Epstein RJ, Stulting RD, Hendricks RL, Harris DM. Corneal neovascularization. Pathogenesis and inhibition. *Cornea*. 1987;6:250–257.
9. Klintworth GK, Burger PC. Neovascularization of the cornea: current concepts of its pathogenesis. *Int Ophthalmol Clin*. 1983;23:27–39.
10. Lu P, Li L, Mukaida N, Zhang X. Alkali-induced corneal neovascularization is independent of CXCR2-mediated neutrophil infiltration. *Cornea*. 2007;26:199–206.
11. Lu P, Li L, Kuno K, et al. Protective roles of the fractalkine/CX3CL1-CX3CR1 axis against alkali-induced corneal neovascularization through enhanced anti-angiogenic factor expression. *J Immunol*. 2008;108:4283–4291.
12. Lu P, Li L, Wu Y, Mukaida N, Zhang X. Essential contribution of CCL3 to alkali-induced corneal neovascularization by regulating vascular endothelial growth factor production by macrophages. *Mol Vis*. 2008;14:1614–1622.
13. Lu P, Li L, Liu G, Van Rooijen N, Mukaida N, Zhang X. Opposite roles of CCR2 and CX3CR1 macrophages in alkali-induced corneal neovascularization. *Cornea*. 2009;28:562–569.
14. Baud V, Karin M. Signal transduction by tumor necrosis factor and its relatives. *Trends Cell Biol*. 2001;11:372–377.
15. Chen G, Goeddel DV. TNF-R1 signaling: a beautiful pathway. *Science*. 2002;296:1634–1635.
16. Rodrigues EB, Farah ME, Maia M, et al. Therapeutic monoclonal antibodies in ophthalmology. *Prog Retin Eye Res*. 2009;28:117–144.
17. Saika S, Ikeda K, Yamanaka O, et al. Loss of tumor necrosis factor alpha potentiates transforming growth factor beta-mediated pathogenic tissue response during wound healing. *Am J Pathol*. 2006;168:1848–1860.
18. Fujita S, Saika S, Kao WW, et al. Endogenous TNFalpha suppression of neovascularization in corneal stroma in mice. *Invest Ophthalmol Vis Sci*. 2007;48:3051–3055.
19. Leibovich SJ, Polverini PJ, Shepard HM, Wiseman DM, Shively V, Nuseir N. Macrophage-induced angiogenesis is mediated by tumour necrosis factor α. *Nature*. 1987;329:630–632.
20. Mahadevan V, Hart IR, Lewis GP. Factors influencing blood supply in wound granuloma quantitated by a new in vivo technique. *Cancer Res*. 1989;49:415–419.
21. Gao B, Saba TM, Tsan MF. Role of α(v)β(3)-integrin in TNF-α-induced endothelial cell migration. *Am J Physiol Cell Physiol*. 2002;283:C1196–C1205.
22. Nakao S, Kuwano T, Ishibashi T, Kuwano M, Ono M. Synergistic effect of TNF-alpha in soluble VCAM-1-induced angiogenesis through alpha 4 integrins. *J Immunol*. 2003;170:5704–5711.
23. Shi X, Semkova I, Müther PS, Dell S, Kociok N, Joussen AM. Inhibition of TNF-alpha reduces laser-induced choroidal neovascularization. *Exp Eye Res*. 2006;83:1325–1334.
24. Theodossiadis PG, Liarakos VS, Sfikakis PP, Vergados IA, Theodossiadis GP. Intravitreal administration of the anti-tumor necrosis factor agent infliximab for neovascular age-related macular degeneration. *Am J Ophthalmol*. 2009;147:825–830.
25. Fujioka N, Mukaida N, Harada A, et al. Preparation of specific antibodies against murine IL-1ra and the establishment of IL-1ra as an endogenous regulator of bacteria-induced fulminant hepatitis in mice. *J Leukoc Biol*. 1995;58:90–98.

26. Ishida Y, Kondo T, Tsuneyama K, Lu P, Takayasu T, Mukaida N. The pathogenic roles of tumor necrosis factor receptor p55 in acetaminophen-induced liver injury in mice. *J Leukoc Biol*. 2004;75:59–67.
27. Mori R, Kondo T, Ohshima T, Ishida Y, Mukaida N. Accelerated wound healing in tumor necrosis factor receptor p55-deficient mice with reduced leukocyte infiltration. *FASEB J*. 2002;16: 963–974.
28. Cursiefen C, Chen L, Saint-Geniez M, et al. Nonvascular VEGF receptor 3 expression by corneal epithelium maintains avascularity and vision. *Proc Natl Acad Sci USA*. 2006;103: 11405–11410.
29. Sakurai E, Anand A, Ambati BK, Van Rooijen N, Ambati J. Macrophage depletion inhibits experimental choroidal neovascularization. *Invest Ophthalmol Vis Sci*. 2003;44:3578–3585.
30. Grossniklaus HE, Ling JX, Wallace TM, et al. Macrophage and retinal pigment epithelium expression of angiogenic cytokines in choroidal neovascularization. *Mol Vis*. 2002;21:119–126.
31. Tsutsumi C, Sonoda KH, Egashira K, et al. The critical role of ocular-infiltrating macrophages in the development of choroidal neovascularization. *J Leukocyte Biol*. 2003;74:25–32.
32. Espinosa-Heidmann DG, Suner IJ, Hernandez EP, Monroy D, Csaky KG, Cousins SW. Macrophage depletion diminishes lesion size and severity in experimental choroidal neovascularization. *Invest Ophthalmol Vis Sci*. 2003;44:3586–3592.
33. Oh H, Takagi H, Takagi C, et al. The potential angiogenic role of macrophages in the formation of choroidal neovascular membranes. *Invest Ophthalmol Vis Sci*. 1999;40:1891–1898.
34. Kociok N, Radetzky S, Krohne TU, Gavranic C, Joussen AM. Pathological but not physiological retinal neovascularization is altered in TNF-Rp55-receptor-deficient mice. *Invest Ophthalmol Vis Sci*. 2006;47:5057–5065.
35. Regatieri CV, Dreyfuss JL, Melo GB, Lavinsky D, Farah ME, Nader HB. Dual role of intravitreous infliximab in experimental choroidal neovascularization. Effect on the expression of sulfated glycosaminoglycans. *Invest Ophthalmol Vis Sci*. 2009; 50:5487–5494.
36. Fiers W, Beyaert R, Boone E, et al. TNF-induced intracellular signaling leading to gene induction or to cytotoxicity by necrosis or by apoptosis. *J Inflamm*. 1995;47:67–75.
37. Moromizato Y, Stechschulte S, Miyamoto K, et al. CD18 and ICAM-1-dependent corneal neovascularization and inflammation after limbal injury. *Am J Pathol*. 2000;157:1277–1281.
38. Zhu SN, Dana MR. Expression of cell adhesion molecules on limbal and neovascular endothelium in corneal inflammatory neovascularization. *Invest Ophthalmol Vis Sci*. 1999;40:1427–1434.
39. Lu P, Li L, Liu G, Zhang X, Mukaida N. Enhanced experimental corneal neovascularization along with aberrant angiogenic factor expression in the absence of IL-1 receptor antagonist. *Invest Ophthalmol Vis Sci*. 2009;50:4761–4768.
40. Popivanova BK, Kitamura K, Wu Y, et al. Blocking TNF-alpha in mice reduces colorectal carcinogenesis associated with chronic colitis. *J Clin Invest*. 2008;118:560–570.
41. Lee H, Baek S, Joe SJ, Pyo SN. Modulation of IFN-gamma production by TNF-alpha in macrophages from the tumor environment: significance as an angiogenic switch. *Int Immunopharmacol*. 2006;6:71–78.
42. Sica A, Mantovani A. Macrophage plasticity and polarization: in vivo veritas. *J Clin Invest*. 2012;1222:787–795.
43. Bystrom J, Evans I, Newson J, et al. Resolution-phase macrophages possess a unique inflammatory phenotype that is controlled by cAMP. *Blood*. 2008;112:4117–4127.
44. Okada Y, Ikeda K, Yamanaka O, et al. TNFalpha suppression of corneal epithelium migration. *Mol Vis*. 2007;13:1428–1435.